

## FINITE ELEMENT ANALYSIS OF A WELDING TRANSFORMER

Antônio Flavio Licarião Nogueira

Santa Catarina State University, Joinville, Santa Catarina, Brazil

### ABSTRACT

The study introduces the detailed sequence of operations necessary to determine the self- and mutual inductances of power transformers from numerically simulated open-circuit and bucking experiments. Parameters of a welding style transformer are compared to those of a normal step-down transformer of equivalent ratings. The investigation identifies the different patterns of magnetic flux circulation when the two transformers operate with rated load. Implications of the high reactance of welding transformers on the consumption of reactive power and power factor are analyzed.

**Keywords:** Inductance, Energy storage, Finite element analysis, Transformer cores, Welding.

### 1. INTRODUCTION

Welding is the process of using heat to join metals. Generally, welding is the preferred joining method, and most common steels are weldable [1]. The most popular welding machines use the arc welding methods. These include: i) the stick welding or shielded metal arc welding (SMAW); ii) the mig welding or gas metal arc welding (GMAW); and iii) the tig welding or gas tungsten arc welding (GTAW). Beyond the three arc welding techniques, there are other important processes to be considered like brazing, soldering and oxyacetylene welding. The resistance spot welding system (RSW) is one of the most efficient material-joining processes in the automobile industry. The RSW process utilizes currents in the range of 1-200 kA with durations ranging from a few cycles to one second to generate Joule heating. RSW transformers operate within a middle-frequency range of around 1 kHz [2]. Some welding systems use low-frequency transformers that operate at the utility mains frequency of 50 or 60 Hz. These systems are the least expensive but the transformers are often bulky and massive.

In many electric welding systems, a potential difference of 50-70 volts is required to strike an electric arc. After the arc is struck, an essentially constant current supply is desired [3]. The welding transformer converts the high voltage and low current from the utility mains into a low voltage and high current, usually in the range of 55 to 590 amperes. In the illustration of figure 1(a), it is presented a cross-sectional view of a conventional step-down transformer wherein the two windings are mounted in separate limbs of the transformer's magnetic core. The transformer shown in figure 1(b) is designed for use in a welder. This special transformer provides a low-reluctance path for the leakage flux between the primary and secondary windings. The low-reluctance path is the result of moving a magnetic shunt in and out of the transformer core.

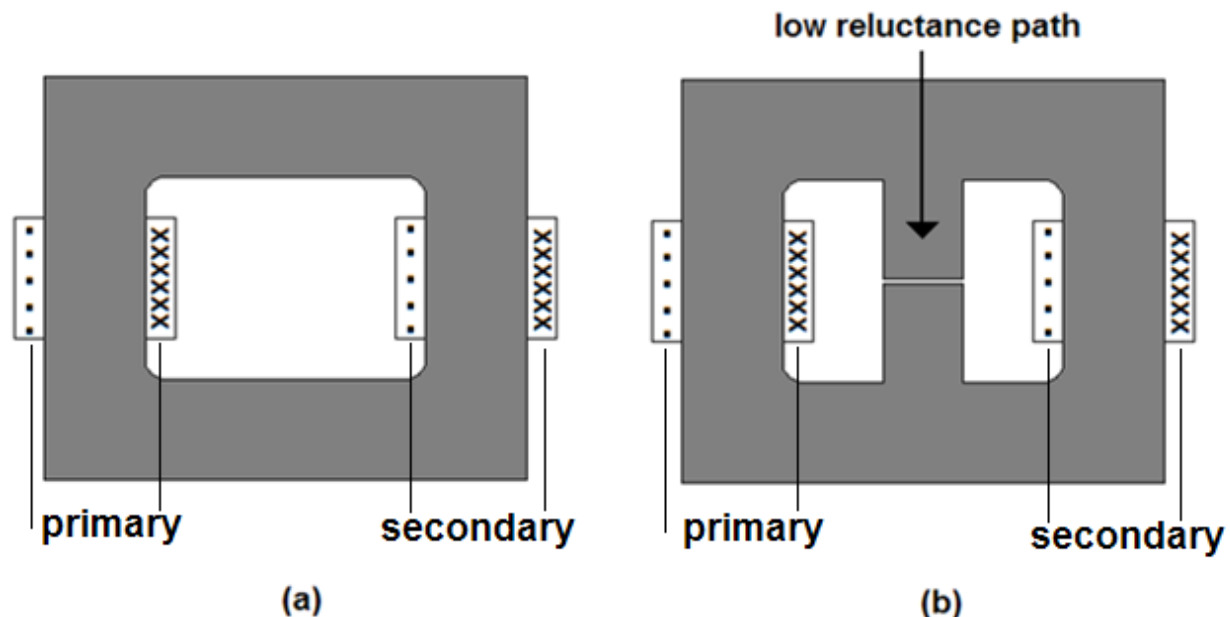


Figure 1. Cross-sectional views: (a) conventional transformer; (b) welding style transformer.

In the present analysis, it is only considered the case of a gapped and fixed magnetic shunt placed in the center of the transformer's window. The inclusion of the magnetic shunt to provide a low-reluctance path substantially alters the circulation of magnetic flux at load operation. In the conventional transformer, a substantial proportion of the total flux produced by each winding follows a path through the outside air, and much noise is propagated outside the transformer. In the illustration of figure 2(a),  $\phi_{tot}$  denotes the total flux generated by the winding magnetomotive force,  $\phi_{int}$  is the flux crossing the transformer's window, and  $\phi_{ext}$  is the flux that passes through the outside air. In the welding transformer shown in figure 2(b), the external flux  $\phi_{ext}$  practically vanishes, and the flux  $\phi_{int}$  that circulates internally, through the central gapped limb, represents almost the entire generated magnetic flux  $\phi_{tot}$ . When compared to a conventional transformer with the same winding specifications such as number of turns, rated currents and voltages, the welding transformer possesses a much higher leakage inductance, and this is the main difference between the two types of transformer. Higher leakage inductance means less fluctuation in the electric current drawn from the power supply over a wide range of load conditions. Due to the higher leakage inductance, the welding style transformer is able to withstand the short-circuit conditions on the welding output side.

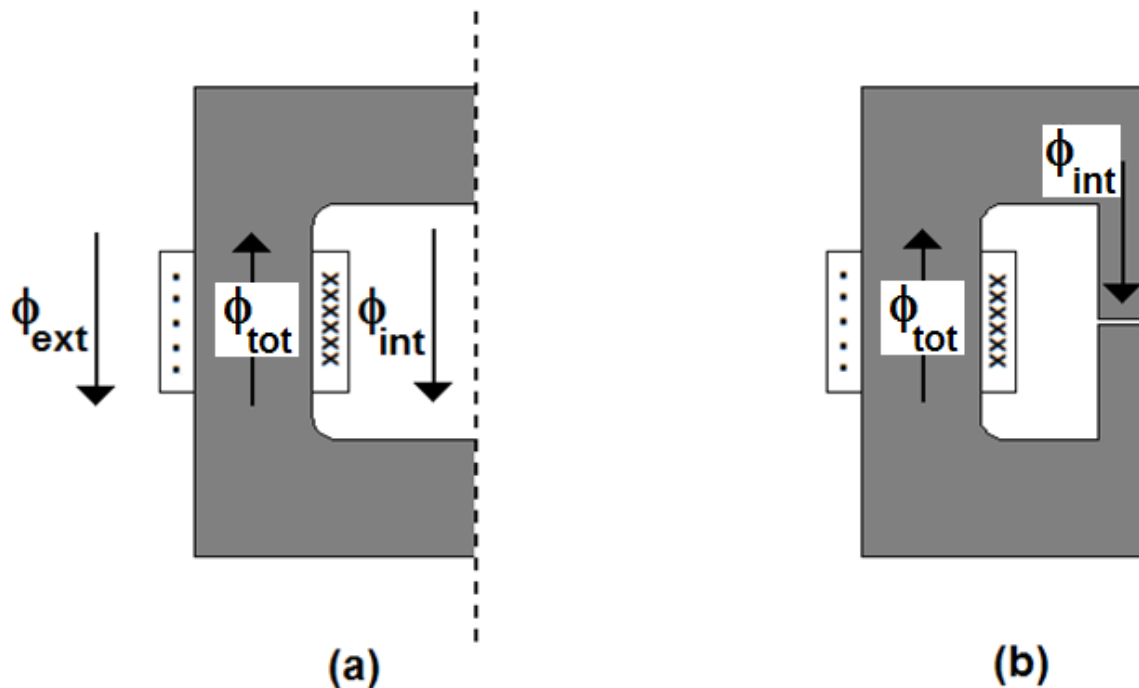


Figure 2. Circulation of magnetic flux on load conditions: (a) conventional transformer; (b) welding style transformer.

In the present study, parameters of a welding style transformer are compared to those of an equivalent conventional transformer with same rated voltages, currents and winding specifications. The investigation is mainly related to the different patterns of circulating fluxes as well as to the determination of the leakage inductance of the two types of transformers. The numerically simulated open- and short-circuit tests to calculate inductances follow the approach described in [4].

## 2. PROBLEM DESCRIPTION

The comparative study involves two different transformers. Both transformers have the same rated voltages, currents and specifications of the windings. The primary windings contain 40 turns and are rated for 162.63 volts; the secondary windings contain 22 turns and are rated for 89.45 volts. The main difference between the two transformers under investigation is the inclusion of a gapped central limb in the welding style transformer. A cross-sectional view of the conventional transformer is presented in figure 3(a), and a cross-sectional view of the welding transformer is presented in figure 3(b). The geometrical details of the transformers' magnetic cores are indicated in figure 3, with the dimensions in centimeter. Rated values of the windings are summarized in table 1.

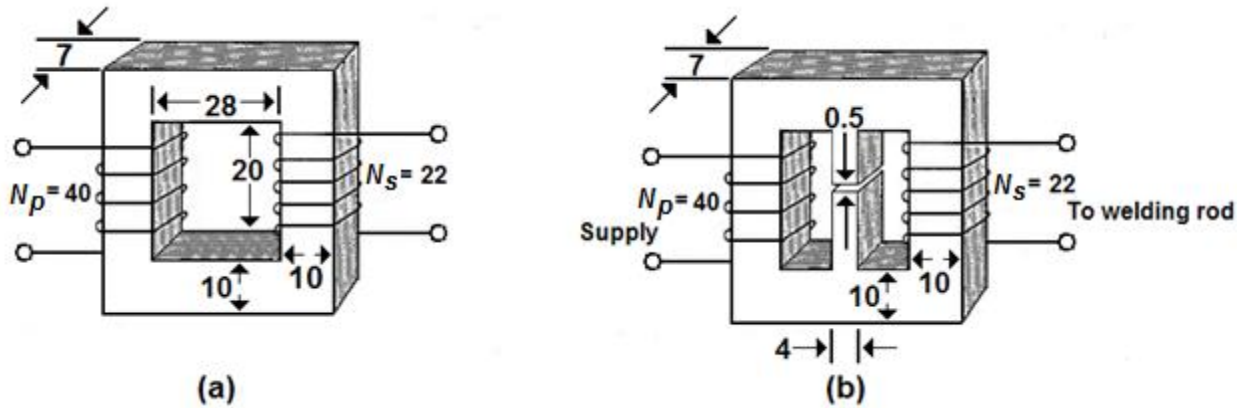


Figure 3. Cross-sectional views: (a)conventional transformer;(b) welding style transformer. Dimensions in centimeter.

Table 1. Rated values of the two windings; annotated voltages and currents represent peak values.

Primary	Secondary
Number of turns, $N_p=40$	Number of turns, $N_s=22$
Voltage, $v_p=162.63$ V	Voltage, $v_s=89.45$ V
Current, $i_p=191.43$ A	Current, $i_s=348.05$ A

The two-dimensional simulation software “finite element method magnetics”(FEMM)has been used to obtain the numerical solutions [5]. This is a current-driven finite-element program that works with prescribed currents rather than voltages.A cross-sectional view of the finite element model is presented in figure 4. The cores of the two idealized transformers are formed by a magnetically linear material, with a constant relative permeability of 1000. The light gray regions  $S_1$ ,  $S_2$  and  $S_3$  that appear in the centre of the draw allow the use of the technique of material re-identification as well as the use of a single finite-element mesh in the different magnetostatic solutions [6]. In the field solutions related to the conventional transformer, the material properties of regions  $S_1$ ,  $S_2$  and  $S_3$  are simply specified as “air”. In the field solutions related to the welding transformer, the material properties of regions  $S_1$  and  $S_3$  are the same of the magnetic core with relative permeability  $\mu_r=1000$ , and the material property of region  $S_2$  is specified as air.

The numerical model includes an external, rectangular boundary not indicated in figure 4. Along the external boundary, the magnetic vector potential  $A$  is made equal to zero. This is a “Dirichlet boundary”, and is used to close the domain of analysis [7]. Each winding is modeled by two non-contiguous rectangular regions, and the properties of these regions include the specification of the coil’s number of turns and terminal current.In addition, each pair of regions representing a stranded coil must be defined as series-connected[8].

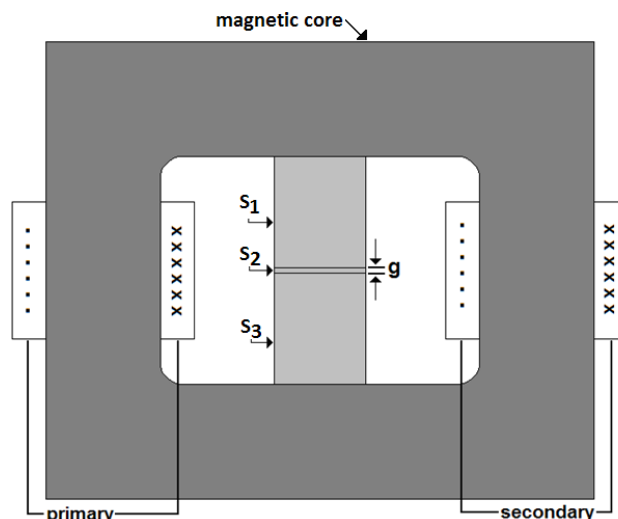


Figure 4. Cross sectional view of the finite element model.

### 3. TRANSFORMER EQUIVALENT CIRCUIT

Consider the transformer equivalent circuit shown in figure 5. The evaluation of the transformer parameters previously discussed in [4] has considered the simple case wherein the windings have equal numbers of turns. In the present study, it is considered the more general case in which the windings may have different number of turns. This equivalent circuit represents a transformer with lossless magnetic core, and only the ohmic loss in the two conductive windings is taken into account. In this circuit,  $R_p$  and  $R_s$  represent the resistance of the primary and secondary windings, respectively. The leakage reactances of the primary and secondary windings are represented by  $x_p$  and  $x_s$ , respectively. The magnetizing reactance is represented by  $X_m$ , and appears in the circuit's vertical branch. Whenever convenient, all quantities may be referred to the primary side of this particular step-down transformer. Secondary voltages and currents must be scaled up and down, respectively, by the turns ratio  $N_p/N_s=1.818$ . Resistances and inductive reactances of the primary and secondary circuits must be related by the rated turns ratio squared,  $[N_p/N_s]^2=a^2=3.306$ .

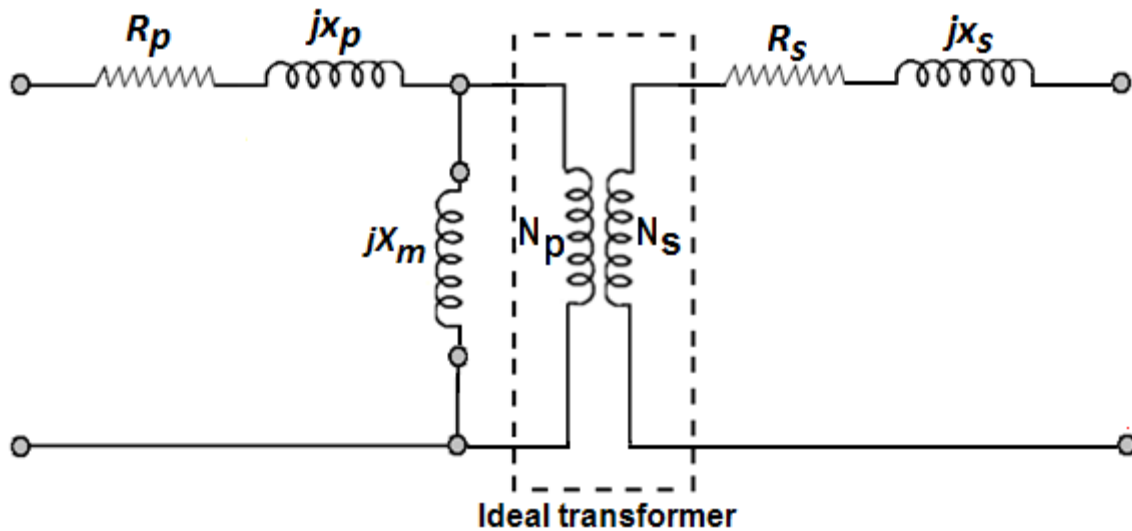


Figure 5. Transformer equivalent circuit.

### 4. OPEN-CIRCUIT AND BUCKING TESTS

#### 4.1. Self-inductance and open circuit test

In the open-circuit test, the secondary is open-circuited, so that the terminal current is  $i_s=0$ . The primary winding carries the steady-state magnetizing current. This is a distorted and periodic current, and its peak value usually represents a small percentage in the range of 1 to 5 per cent of the winding full-load current [9]. In the present magnetostatic analysis, the effect of the magnetizing current is simulated by specifying a direct current  $i_p=1.9143$  A that represents 1.0 per cent of the primary current peak value.

The simulated open-circuit test is used to determine the total primary reactance  $x_p + X_m$ . Specification of primary currents and number of turns for the open-circuit test is summarized in table 2. In this particular simulation, a magnetomotive force of 76.572 ampere-turns is applied to each transformer magnetic core.

Table 2. Specification of currents for the open-circuit test.

Primary coil				
Terminal current (A)	Number of turns		Total current (A)	
	Left end-side	Right end-side	Left end-side	Right end-side
1.9143	-40	+40	-76.572	76.572

#### 4.2. Mutual inductance and stored energies

The mutual inductance in a two-winding system may be determined by a difference measurement involving two tests, one with the two winding currents oriented to have their fluxes adding, the other with the fluxes bucking each other [10]. If  $W_a$  denotes the magnetically stored energy of the first test and  $W_b$  the energy stored in the second one, the system's mutual inductance  $M$  referred to the primary circuit is

$$M = \frac{W_a - W_b}{2(i_p)(i_{sp})}, \quad (1)$$

where  $i_p$  is the primary current and  $i_{sp}$  is the secondary current referred to the primary circuit. The two currents  $i_s$  and  $i_{sp}$  are numerically equal.

Specification of the direct currents and winding connections related to the experiment wherein the two winding currents are oriented to have their fluxes adding is summarized in table 3. Information related to the experiment wherein the two winding currents are oriented to have their fluxes bucking each other is summarized in table 4.

Table 3. Specification of currents and winding connections for the experiment with adding fluxes.

Primary coil			Secondary coil		
Terminal current (A)	Specified number of turns		Terminal current (A)	Specified number of turns	
	Left-end side	Right-end side		Left-end side	Right-end side
191.43	-40	+40	348.05	+22	-22

Table 4. Specification of currents and winding connections for the experiment with the fluxes bucking each other.

Primary coil			Secondary coil		
Terminal current (A)	Specified number of turns		Terminal current (A)	Specified number of turns	
	Left-end side	Right-end side		Left-end side	Right-end side
191.43	-40	+40	348.05	-22	+22

## 5. INDUCTANCE CALCULATIONS

In the following, it is presented the sequence of numerical operations required to calculate self- and mutual inductances of the conventional transformer. Inductance calculations for the welding transformer are presented in the Appendix.

### 5.1. Self-inductance calculations

The magnetostatic solutions that represent the open-circuit test are used to determine the self-inductances of the two windings using the energy approach [11]. When the terminal current of the 40-turn primary winding is  $i_p=1.9143$  A, the total magnetic energy stored in the modeled domain is  $W=22.4507$  mJ. The self-inductance  $L_p$  of the primary winding is calculated by

$$L_p = \frac{2W}{(i_p)(i_p)} = \frac{2(0.0224507)}{(1.9143)^2} = 12.2529 \text{ mH}. \quad (2)$$

When the terminal current of the 22-turn secondary winding is 3.4805 A, the total magnetic energy stored in the modeled domain is  $W=22.4551$  mJ. The self-inductance  $L_s$  of the secondary winding is given by

$$L_s = \frac{2W}{(i_s)(i_s)} = \frac{2(0.0224551)}{(3.4805)^2} = 3.7073 \text{ mH}. \quad (3)$$

Computed self-inductances  $L_p$  and  $L_s$  are correctly related by the turns-ratio squared, i.e.,

$$\frac{L_p}{L_s} = 3.306 \cong \left(\frac{40}{22}\right)^2. \quad (4)$$

### 5.2. Mutual inductance calculations

The calculation of mutual inductances is based in two experiments wherein both windings carry currents. In this particular analysis, the terminal direct currents of the primary and secondary windings are equal to the peak values of the rated currents, to know,  $i_p=191.43$  A and  $i_s=348.05$  A, respectively. In the illustration of figure 5,  $\phi_p$  denotes the flux generated by current flowing in the primary winding and  $\phi_s$  denotes the flux generated by current flowing in the secondary winding.

In the experiment illustrated in figure 5(a), the two winding currents are oriented to have their fluxes adding. In this simulated experiment, the magnetic stored energy is  $W_a=891.313$  J. In the experiment illustrated in figure 5(b), the

two winding currents are oriented to have their flux bucking each other, and the magnetic stored energy is  $W_b=6.80253$  J. The mutual inductance  $M_p$ , referred to the 40-turn primary circuit is

$$M_p = \frac{891.313 - 6.80253}{2(191.43)(191.43)} = 12.0685 \text{ mH.} \quad (5)$$

The mutual inductance  $M_s$ , referred to the 22-turn secondary circuit is

$$M_s = \frac{891.313 - 6.80253}{2(348.05)(348.05)} = 3.6508 \text{ mH.} \quad (6)$$

The ratio of computed mutual inductances is  $M_p/M_s=3.306$ , equal to the rated turns-ratio squared.

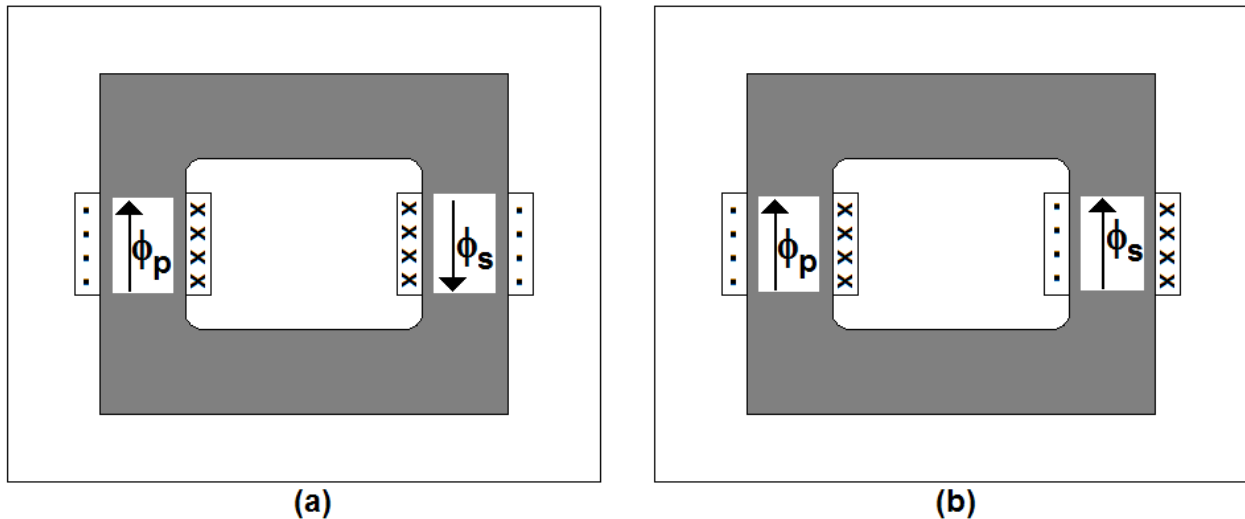


Figure 6. Orientation of winding currents; (a) fluxes adding; (b) fluxes bucking each other.

### 5.3. Leakage inductance calculations

If  $L_p$  denotes the total or self-inductance of the primary winding, and  $M_p$  denotes the transformer's mutual inductance referred to the primary side, the leakage inductance  $l_p$  of the primary winding is given by the subtraction,

$$l_p = L_p - M_p = 0.1844 \text{ mH.} \quad (7)$$

In a similar fashion, the leakage inductance  $l_s$  of the secondary winding is given by

$$l_s = L_s - M_s = 0.0566 \text{ mH.} \quad (8)$$

The ratio of computed leakage inductances is  $l_p/l_s=3.26$ , close to the rated turns-ratio squared.

## 6. COMPARATIVE STUDY

### 6.1. Equivalent circuits

Consider the simplified equivalent circuits presented in figure 7. The equivalent circuit of the conventional transformer appears in figure 7(a), and the equivalent circuit of the welding transformer is shown in figure 7(b). All inductive reactances in these diagrams are related to an operating frequency of 60 hertz with numerical values in milliohm.

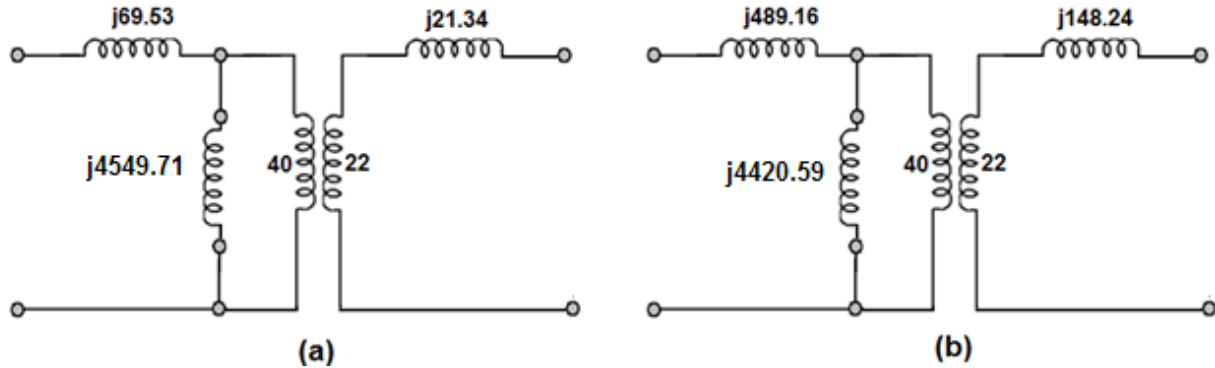


Figure 7. Equivalent circuits; (a) conventional transformer; (b) welding transformer. Reactance values in milliohm.

A close observation of the two equivalent circuits clearly shows that the welding transformer possesses much higher leakage reactances. The leakage reactances of the welding transformer are seven times greater than those of the conventional transformer. This has clear implications on the transformers' performance in terms of power consumption and power factor.

Time-harmonic finite element analyses at a frequency of 60 hertz have been used to simulate the operation with rated load. In these simulations, the two winding currents are oriented to have their flux bucking each other. The peak value of the primary current is  $i_p=191.43$  A, and the peak value of the secondary current is  $i_s=348.05$  A. Results from the operation with rated load show that both transformers draw from the supply network the same mean real power, to know,  $P=2.148$  kW. The consumption of reactive power, on the other hand, differs considerably. Whilst the consumption of reactive power of the conventional transformer is 1.274 kvar, the consumption of the welding transformer is 8.963 kvar, seven times greater. This has a clear consequence on the power factor. Whereas the conventional transformer represents a 0.86 power-factor load, the welding transformer represents a very low 0.23 power-factor load.

The high reactance of welding transformers limits the fluctuations of the transformer current but each welder represents a low power factor load. With several welders working simultaneously, these lagging power factor loads can create a significant voltage drop and unbalanced load conditions for the power system. Methods for improving the power quality on the welding circuits of industrial power distribution systems are discussed in [12], [13] and [14].

## 6.2. Flux density distributions

### 6.2.1. No-load operation

The flux density distributions for the two transformers' open-circuit operating condition are shown in figure 8.

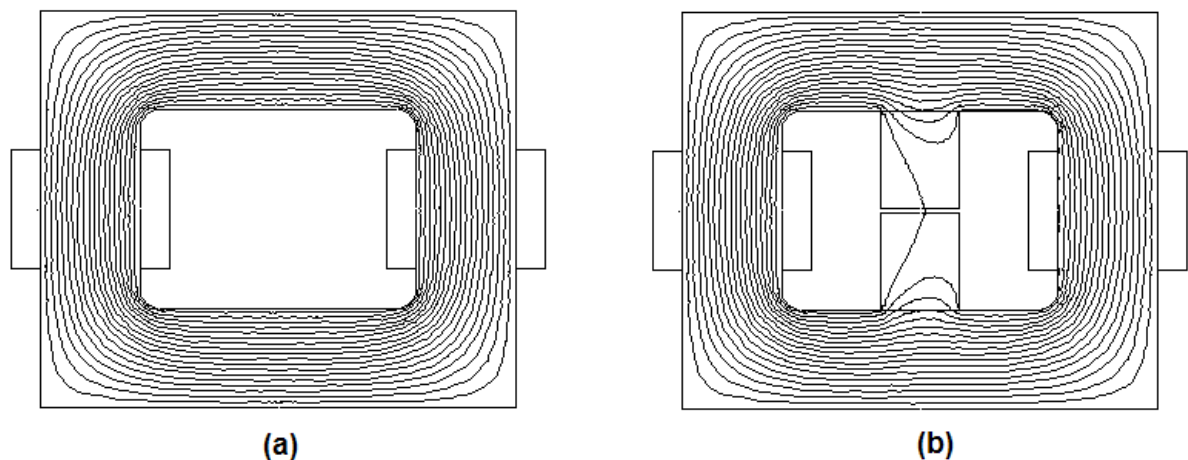


Figure 8. Flux lines for the no-load operating condition; (a) conventional transformer; (b) welding transformer.

With the aid of these plots, it is possible to observe that, in both cases, the magnetic fluxes are mainly confined to the magnetic cores. In the conventional transformer, the storage of magnetic field energy in the magnetic core represents 98.9% of the system's stored energy. In the welding transformer, the storage of magnetic field energy in the magnetic core, including the magnetic shunt, represents 95.1% of the system's stored energy.

### 6.2.2. On-load operation

The plots of the flux density distribution for the two transformers operating with rated load are shown in figure 9. In both magnetostatic field solutions the two winding currents are oriented to have their flux bucking each other. The *dc*-value of the primary current is  $i_p=191.43$  A, and the *dc*-value of the secondary current is  $i_s=348.05$  A.

Examination of the flux distributions reveals that, in the conventional transformer, a substantial proportion of the total flux produced by each winding follows a path through the outside air, and much noise is propagated outside the transformer. In the welding transformer, on the other hand, the external flux circulation practically vanishes. In this style of transformer, the flux generated by each winding circulates internally, following a path through the central magnetic shunt.

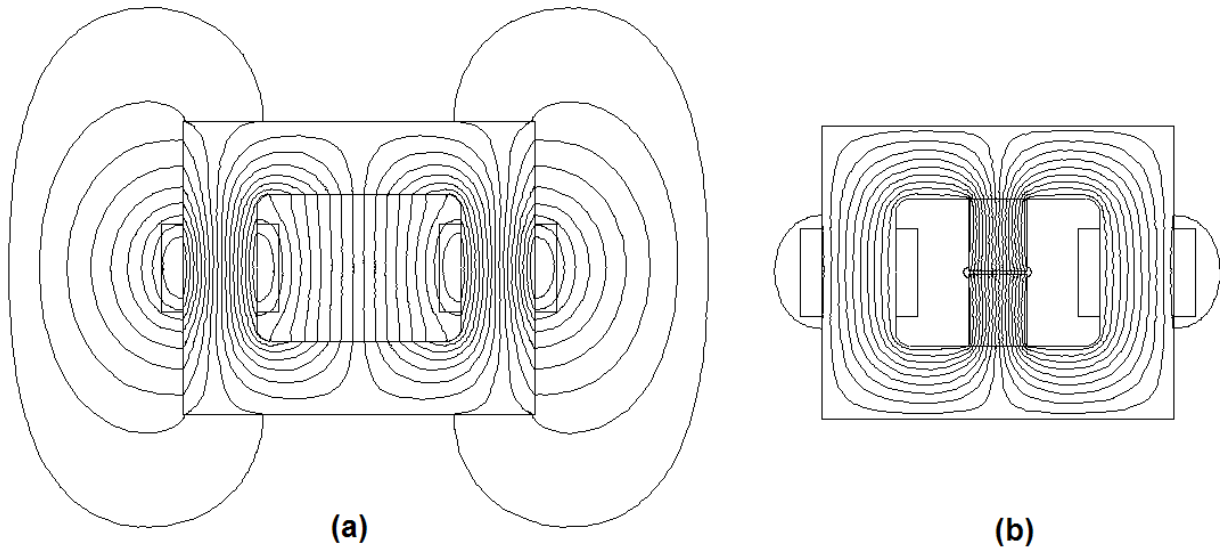


Figure 9. Flux lines for operation at rated load condition; (a) conventional transformer; (b) welding transformer.

## 7. APPENDIX

### INDUCTANCE CALCULATIONS OF THE WELDING TRANSFORMER

In the following, it is presented the sequence of numerical operations required to calculate self- and mutual inductances of the welding transformer.

#### A.1. Self-inductance calculations

The field solutions that represent the open-circuit test are used to determine the self-inductance of the two windings using the energy approach. When the terminal current of the 40-turn primary winding is  $i_p=1.9143$  A, the total magnetic energy stored in the modeled domain is  $W=23.8626$  mJ. The self-inductance  $L_p$  of the primary winding is calculated by

$$L_p = \frac{2W}{(i_p)(i_p)} = \frac{2(0.0238626)}{(1.9143)^2} = 13.0235 \text{ mH.} \quad (\text{A-1})$$

When the terminal current of the 22-turn secondary winding is 3.4805 A, the total magnetic energy stored in the modeled domain is  $W=23.8668$  mJ. The self-inductance  $L_s$  of the secondary winding is given by

$$L_s = \frac{2W}{(i_s)(i_s)} = \frac{2(0.0238668)}{(3.4805)^2} = 3.9404 \text{ mH.} \quad (\text{A-2})$$

Computed self-inductances  $L_p$  and  $L_s$  are correctly related by the turns-ratio squared, i.e.,

$$\frac{L_p}{L_s} = 3.305 \cong \left(\frac{40}{22}\right)^2. \quad (\text{A-3})$$



### A.2. Mutual inductance calculations

In this particular analysis, the terminal *dc* currents of the primary and secondary windings are numerically equal to the peak values of the rated currents, to know,  $i_p=191.43$  A and  $i_s=348.05$  A, respectively. In the experiment wherein the two winding currents are oriented to have their fluxes adding, the magnetic stored energy is  $W_a=906.997$  J. In the experiment wherein the two winding currents are oriented to have their fluxes bucking each other, the magnetic stored energy is  $W_b=47.5903$  J. The mutual inductance  $M_p$ , referred to the 40-turn primary circuit is

$$M_p = \frac{906.997 - 47.5903}{2(191.43)(191.43)} = 11.7260 \text{ mH.} \quad (\text{A-4})$$

The mutual inductance  $M_s$ , referred to the 22-turn secondary circuit is

$$M_s = \frac{906.997 - 47.5903}{2(348.05)(348.05)} = 3.5472 \text{ mH.} \quad (\text{A-5})$$

Computed mutual inductances are correctly related by the turns ratio squared.

### A.3. Leakage inductance calculations

If  $L_p$  denotes the total or self-inductance of the primary winding, and  $M_p$  denotes the transformer's mutual inductance referred to the primary side, the leakage inductance  $l_p$  of the primary winding is given by the subtraction,

$$l_p = L_p - M_p = 1.2975 \text{ mH.} \quad (\text{A-6})$$

In a similar fashion, the leakage inductance  $l_s$  of the secondary winding is given by

$$l_s = L_s - M_s = 0.3932 \text{ mH.} \quad (\text{A-7})$$

The ratio of computed leakage inductances is  $l_p/l_s=3.26$ , and this is close to the rated turns-ratio squared.

## 8. CONCLUSIONS

In the present study, the leakage reactances of a welding style transformer are compared to those of a normal step-down transformer of equivalent ratings. The paper explains how to use static numerical field solutions to compute the self- and mutual inductances of power transformers. Open-circuit tests are used to determine the self-inductance of the transformers windings, and bucking tests are used in the calculation of mutual inductances. A unique finite-element model has been used in all computations. During the pre-processing stage, the most important feature is the correct specification of current flow directions in the regions that represent the end-sides of the transformers' windings. At the post-processing stage, the most important task is the calculation of self- and mutual inductances from the numerical field solutions. The investigation identifies the different patterns of magnetic flux circulation when the two transformers operate with rated load. Results from the operation with rated load help to understand the effects of the high reactance of welding transformers on the consumption of reactive power and power factor.

## 9. ACKNOWLEDGEMENT

The author gives thanks to David Meeker (dmeeker@ieee.org) for the use of the finite element CAD system FEMM. The author also gives thanks to the Brazilian Federal Agency for Postgraduate Studies (CAPES) for the sponsored access to several scientific web sites.

## 10. REFERENCES

- [1]. Z. Boumerzoug, C. Derfouf, Thierry Baudin, "Effect of welding on microstructure and mechanical properties of an industrial low carbon steel", *Engineering*, doi: 10.4236/eng.2010.27066
- [2]. V. Podlogar, B. Klopčič, G. Stumberger, and D. Dolinar, "Magnetic core model of a midfrequency resistance spot welding transformer", *IEEE Trans. on Magnetics*, doi: 10.1109/TMAG.2009.2031979
- [3]. G.R. Slemon and A. Straughen, *Electric machines* (Addison Wesley Publishing Company, London, 1982), pp. 172.
- [4]. A.F.L. Nogueira, "Calculation of power transformers equivalent circuit parameters using numerical field solutions", *International Journal of Research and Reviews in Applied Sciences*, **17**(1) October 2013.
- [5]. D. Meeker, *Finite element method magnetics, user's manual*.
- [6]. Available: <http://www.femm.info/Archives/doc/manual42.pdf>

- 
- [7]. A.F.L. Nogueira, “Computation of magnetic forces in moving coil drivers using mean and difference potentials”, *International Journal of Research and Reviews in Applied Sciences*, **13**(2) 398-405 November 2012.
- [8]. A.F.L. Nogueira, “A case study on open boundary techniques for electromagnetic field problems with translational symmetry”, *Journal of Microwaves, Optoelectronics and Electromagnetic Applications*, **9**(1) 20-33 (2010).
- [9]. A.F.L. Nogueira and L.J.A.S. Maldonado, “Analysis of AC contactors combining electric circuits, time-harmonic finite element simulations and experimental work”, *International Journal of Research and Reviews in Applied Sciences*, **14**(3) 513-525 (2013).
- [10]. A.F.L. Nogueira, G.G. Facchinello, and L.A. Ramos, “Prediction of magnetizing currents in power transformers using numerically simulated open-circuit tests”, *International Journal of Research and Reviews in Applied Sciences*, **17**(2) November 2013.
- [11]. D.A. Lowther and P.P. Silvester, *Computer-aided design in magnetics* (Springer-Verlag, New York, 1986), pp. 188.
- [12]. A.F.L. Nogueira, “Techniques for two-dimensional finite-element inductance computation”, *International Journal of Research and Reviews in Applied Sciences*, **15**(2) 168-176 (2013).
- [13]. T.L. Baldwin and T. Hogans, “Reactive-power compensation for voltage control at resistance welders”, *IEEE Trans. on Industry Applications*, doi: 10.1109/TIA.2005.858301
- [14]. B. Klopčič, D. Dolinar and G. Stumberger, “Advanced control of a resistance spot welding system”, *IEEE Trans. on Power Electronics*, doi: 10.1109/TPEL.2007.911851
- [15]. G. Stumberger, B. Klopčič, D. Dezelak, and D. Dolinar, “Prevention of iron core saturation in multi-winding transformers for dc-dc converters”, *IEEE Trans. on Magnetics*, doi: 10.1109/TMAG.2009.2031687